

Q1

Design and Analysis of Wing/Winglet Combinations Including Viscous Effects at Low Speeds

Jean-Jacques Chattot*

University of California, Davis, Davis, California 95616

The design and analysis of winglets is presented from an aerodynamic point of view. The winglets considered are small fences placed upward at the tip of the wing to improve the wing efficiency by decreasing the induced drag for a given lift. Viscous corrections are accounted for by using a two-dimensional viscous polar, with the assumption that at design conditions the flow is fully attached. The comparison of the inviscid and viscous designs indicates that viscosity has little effect on the optimum geometry. In the presence of viscous drag, the winglets produce a small thrust; due to viscosity, the overall efficiency gain is decreased. The effect of a small yaw angle on a wing equipped with such optimal winglets indicates that, even in the presence of viscous effects, they provide weathercock stability.

Nomenclature

a	=	winglet height parameter
\mathcal{AR}	=	wing aspect ratio
b	=	wingspan, m
c, c_m	=	chord and root chord parameters
d_m	=	relative camber
e	=	Oswald efficiency factor
F	=	objective function
j_x	=	maximum number of points on wing and winglets
q_n	=	normal wash parameter
s	=	curvilinear abscissa
t	=	angle of twist
U	=	incoming flow velocity, m/s
w_{ind}	=	downwash parameter
x, y, z	=	Cartesian coordinates
α, α_{eff}	=	geometric and effective angles of attack
α_0	=	incidence of zero lift
Γ	=	circulation
$\delta\Gamma$	=	arbitrary circulation variation
κ	=	scaling factor
λ	=	Lagrange multiplier
σ	=	curvilinear abscissa

Subscripts

i	=	inviscid
m	=	main wing
v	=	viscous
w	=	winglet

Introduction

PRANDTL lifting line theory has been used to analyze wing/winglet combinations and, in inverse mode, to help design wings and winglets for practical low-speed aircraft applications.¹ Previous papers have been devoted to winglet design since the early work of Munk,² who investigated the optimum distribution of lifting elements to achieve minimum induced drag, for single dihedral lines

of arbitrary shape as well as multiple lifting lines. Whitcomb³ and Ishimitsu⁴ used a combination of theoretical and experimental work to achieve and validate a practical design. A vortex lattice method was used to search for a low-induced-drag design in both cases, but it is not clear if the procedure provided the optimum solution. Furthermore, the problem complexity was increased by the high subsonic speed range of interest in these studies and the presence of compressibility effects and even shocks.

The first part is a brief recall of the approach and notation for the inviscid aerodynamic optimization of a wing with upward winglets placed at the tip of the wing, using the lifting line theory.⁵ However, the method is more general and is applicable to other wing/winglet dihedral shapes. In the second part, a viscous correction based on the two-dimensional viscous polar is presented. This follows the same lines as work that has been done for wind turbines,⁶ with some differences that are highlighted. A wing with 25% winglet configuration is designed and analyzed at the design condition and the effects of viscosity are assessed. The same configuration is then analyzed for a 1-deg yaw angle in the third part. The inviscid result concerning weathercock stability is extended to the case of viscous flow for small yaw angles.

Inviscid Design and Analysis

Winglets are aerodynamic components placed at the tip of a wing to improve its efficiency in cruise. During the design step, the viscous effects are expected to have a small effect on the optimum distribution of circulation and on the optimum geometry, as was found in the study of optimum wind turbine blades.⁶ In the analysis, however, viscous effects need to be taken into account if the off-design conditions are severe enough. The winglets considered here are perpendicular to the wingspan and oriented upward—hence, they do not contribute to lift—but the method is general and can treat arbitrary dihedral shapes. We make use of the lifting line theory and assume that the wing is of moderate to high aspect ratio and that the Reynolds number is large. A linear two-dimensional lift curve, that is, $C_l(\alpha) = 2\pi(\alpha - \alpha_0)$, is acceptable for the design if the target lift coefficient, $C_{L,target}$, is far from the maximum lift coefficient of the airfoil, where $\alpha_0 = -2d_m - t$ represents the lift at zero incidence which depends on mean relative camber d_m and twist or setting angle t . If this is not the case, a nonlinear lift curve, as given for example by XFOIL,⁷ is used.

To find the wing/winglet combination that corresponds to the minimum induced drag for a given lift, the following objective function, $F = C_{Di} + \lambda C_L$, is defined, where C_{Di} is the drag induced coefficient, λ is the Lagrange multiplier that governs the target lift, and C_L is the lift coefficient and is added to the objective function as a means of enforcing the lift constraint. Let a be the dimensionless winglet height normalized by the semispan, $b/2$. The lift and induced drag

Received 31 December 2004; revision received 3 March 2005; accepted for publication 3 March 2005. Copyright © 2005 by the American Institute of Aeronautics and Astronautics, Inc. All rights reserved. Copies of this paper may be made for personal or internal use, on condition that the copier pay the \$10.00 per-copy fee to the Copyright Clearance Center, Inc., 222 Rosewood Drive, Danvers, MA 01923; include the code 0021-8669/05 \$10.00 in correspondence with the CCC.

*Professor, One Shields Avenue, Mechanical and Aeronautical Engineering. Member AIAA.

coefficients are

$$C_L = \frac{\mathcal{AR}}{2} \int_{-1-a}^{1+a} \Gamma(\sigma) \frac{dy}{d\sigma} d\sigma \quad (1)$$

$$C_{Di} = -\frac{\mathcal{AR}}{2} \int_{-1-a}^{1+a} \Gamma(\sigma) q_n(\sigma) d\sigma \quad (2)$$

where σ (and s) is the curvilinear abscissa along the dihedral shape ($y(s)$, $z(s)$) and q_n is the induced velocity component perpendicular to the dihedral line in the $x = 0$ plane; $q_n = w$ is the usual downwash along the wing, $q_n = v$ on the left winglet, and $q_n = -v$ on the right winglet. The “normal wash,” q_n , depends linearly on Γ as

$$Q2 \quad q_n(s) = -\frac{1}{4\pi} \int_{-1-a}^{1+a} \Gamma'(\sigma) \times \frac{[y(s) - y(\sigma)](dy/ds) + [z(s) - z(\sigma)](dz/ds)}{[y(s) - y(\sigma)]^2 + [z(s) - z(\sigma)]^2} d\sigma \quad (3)$$

where the integral is taken as being “principal valued.” In the numerics, the vortices are placed at $y(\sigma_k)$, between the control points located at $y(s_j)$, and the summation that is substituted to the integral is well behaved.⁸

The quantities have been made dimensionless with the half span, $b/2$, and the incoming flow velocity aligned with the x axis, U . The area of reference is the main wing area A_m . The minimization equation used to solve for the circulation is obtained by taking the Frechet derivative of the objective function, which gives

$$\frac{\partial F}{\partial \Gamma}(\delta\Gamma) = \frac{\partial C_{Di}}{\partial \Gamma}(\delta\Gamma) + \lambda \frac{\partial C_L}{\partial \Gamma}(\delta\Gamma) = 0 \quad \forall \delta\Gamma \quad (4)$$

The boundary conditions are $\Gamma(-1-a) = \Gamma(1+a) = 0$. Since C_{Di} is homogeneous of degree two in Γ and of degree one in C_L , the minimization equation is linear nonhomogeneous in Γ when $\lambda \neq 0$. The solution is obtained in two steps: first the Lagrange multiplier is set to an arbitrary nonzero value, say $\lambda = 1$, and the corresponding circulation and lift C_L are calculated. Then the final answer is obtained by multiplying the circulation by $\kappa = C_{Ltarget}/C_L$. The discrete formulation can be found in Ref. 8, where the cases of a wing without winglets and with 15% winglets and $C_{Ltarget} = 1$ have been treated. The well-known result of an elliptic loading and constant downwash is recovered accurately in the former and a constant downwash and zero sidewash on the winglets with a Oswald efficiency factor $e = 1.17$ results in the latter. This formulation is easily extended to account for viscous effects, as will be shown.

The efficiency is in good agreement with that estimated by Kuhlman and Liaw⁹ and Lundry and Lissaman for vertical winglets, from analysis in the Trefftz plane. The efficiency factor e is defined as the ratio of induced drag coefficient for an elliptically loaded planar wing to the induced drag coefficient of the optimal nonplanar wing/winglet configuration having an equal projected span at equal lift coefficient.

As a test case, a wing with 25% vertical winglets is designed and analyzed for a lift coefficient $C_{Ltarget} = 1$. The results for the circulation and normal wash are shown as solid symbols in Fig. 1. The computation uses a linear lift curve and a fine mesh of $j_x = 101$ points, including the winglets, with a cosine distributions of points on each element. This is required because the normal induced velocity is singular at the wing/winglet junction and small mesh steps are needed there. It can be noted that the winglets do not contribute to the induced drag because the normal induced velocity q_n is zero at the winglets, which is in agreement with the theory.² The winglets are loaded, although much less than the wing. Their role is to redistribute the loads on the wing and decrease the induced drag by lowering the root circulation and by increasing it near the wing/winglet junction. The downwash on the wing is again constant, but of smaller absolute value compared to the elliptic loading.

In inviscid flow theory, there is an infinite number of wings and winglets that will produce the optimum loading. They differ by chord, camber, and twist. In the design step, a constant relative

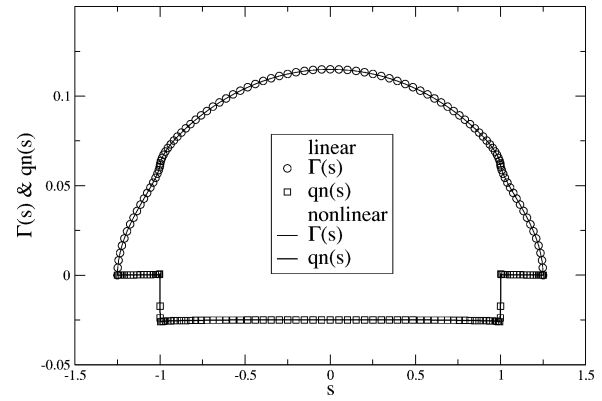


Fig. 1 Circulation and normal wash distributions for optimum wing/winglet combination at design $C_{Ltarget} = 1$ for linear and nonlinear lift curves.

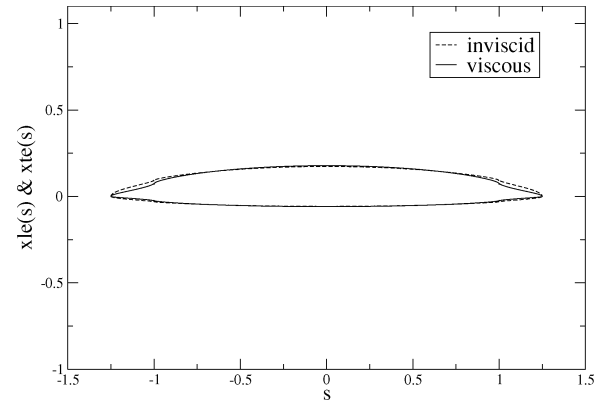


Fig. 2 Wing and winglet chord distribution vs curvilinear abscissa.

camber, $d_m = 0.086$, has been selected for the wing to achieve, for example, high lift coefficient $C_L = 2$ at off-design low-speed condition and maximum efficiency at a cruise lift coefficient of $C_L = 1$. This is in contrast to the optimization of turbine blades where the optimum value of C_l , corresponding to maximum C_l/C_d for the blade, was used in each cross section. The winglets have zero camber. The wing and winglets have no twist. The wing chord distribution is chosen proportional to the circulation; that is, $c(\sigma) = c_m \Gamma(\sigma) / \Gamma(0)$. The wing has an aspect ratio $\mathcal{AR} = 10$ obtained with a maximum root chord $c_m = 0.23$. On the other hand, the chord distribution for the winglets is calculated from $c(\sigma) = 2\Gamma(\sigma) / C_{lw}$, where $C_{lw} \leq (C_{lw})_{max}$ is a design value of the lift coefficient from the winglet lift curve, preferably the value corresponding to maximum C_l/C_d . Here, the value $C_{lw} = 1$ was chosen. The wing and winglet geometry is displayed in Fig. 2, as a dashed line, as if the winglets had been rotated to be a continuation of the wing. The winglets are set with a toe-in angle of $\beta = C_{lw} / (2\pi) = 9.1$ deg. Indeed, with this design choice, the local lift coefficient is constant and equal to the total lift, $C_L = C_l = 2\Gamma(0) / c_m$ on the wing and $C_l = C_{lw}$ on the winglets. The efficiency factor is found to be $e = 1.27$.

The analysis code solves the Prandtl integrodifferential equation. The design geometric incidence angle is given by $\alpha = \alpha_{eff} - \arctan(w_{ind}) = 0.7$ deg. The optimization and analysis codes are in excellent agreement at the design point. The main difference between the two results lies in the normal induced velocity at the wing/winglet junction, which exhibits a strong singularity in the optimization code³ and just a rapid transition in five or six points in the analysis code, the latter being shown in Fig. 1. The induced drag coefficients are for the main wing $(C_{Di})_m = 0.025$ and for the winglets $(C_{Di})_w = 0.00001$, essentially zero to roundoff error.

The same design and analysis are also performed with nonlinear lift curves corresponding to an 8.6% cambered profile for the main wing and a symmetric profile for the winglets, obtained using XFOIL (Fig. 3). The results are also presented in Fig. 1. The optimum distributions of lift and normal wash are the same, as

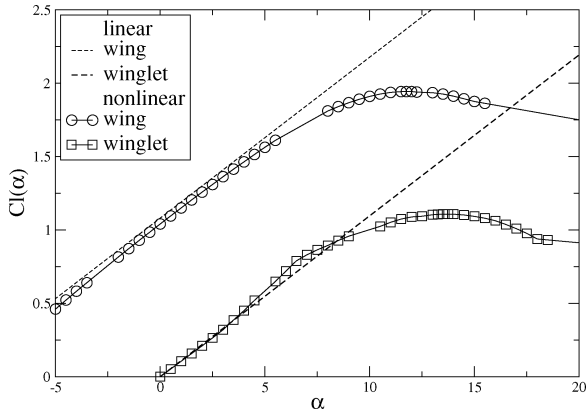


Fig. 3 Lift curves for design and analysis.

expected. The differences are the angles of incidence and toe-in angles at the design point, which for $C_L = 1$ are, respectively, $\alpha = 1.1$ deg and $\beta = 6.5$ deg.

Viscous Correction

Viscous effects can be taken into account, assuming that the flow remains attached everywhere at the design conditions and that strip theory is applicable. A flat-plate approximation can be used or, better, a two-dimensional viscous polar from XFOIL. The viscous contribution must be added to the inviscid induced drag C_{Di} . The viscous drag coefficient is approximated globally or locally by a parabolic distribution, depending on whether a flat-plate formula or a viscous polar is used⁶:

$$C_d(C_l) = C_{d0} + C_{d1}C_l + C_{d2}C_l^2 \quad (5)$$

In the case of a flat-plate formula, the following simple model is used with $C_{d0} = 2C_f$, $C_{d1} = 0$, and $C_{d2} = 2C_{d0}$, where C_f is the friction coefficient of the flat plate of chord c_m . The total viscous drag can be written accordingly:

$$C_{Dv} = \frac{\mathcal{AR}}{4} \int_{-1-a}^{1+a} C_d(\sigma)c(\sigma) d\sigma = C_{Dv0} + C_{Dv1} + C_{Dv2} \quad (6)$$

where the terms are independent, linear, and quadratic in Γ , respectively.

The minimization proceeds as before, with the addition of the term

$$\frac{\partial C_{Dv}}{\partial \Gamma}(\delta\Gamma)$$

where use is made of the relation $dC_d/d\Gamma = (dC_d/dC_l)(dC_l/d\Gamma) = 2(C_{d1} + 4C_{d2}\Gamma/c)/c$, showing that C_{d1} and C_{d2} contribute to the minimization, not C_{d0} . The full minimization equation reads as follows:

$$\begin{aligned} & -\frac{\mathcal{AR}}{2} \int_{-1-a}^{1+a} \left[\delta\Gamma q_n(\sigma) + \Gamma(\sigma) \frac{\partial q_n}{\partial \Gamma}(\delta\Gamma) \right] d\sigma \\ & + \frac{\mathcal{AR}}{2} \int_{-1-a}^{1+a} \delta\Gamma \left[C_{d1} + \frac{4C_{d2}}{c(\sigma)} \Gamma(\sigma) \right] d\sigma \\ & + \lambda \frac{\mathcal{AR}}{2} \int_{-1-a}^{1+a} \delta\Gamma \frac{dy}{d\sigma} d\sigma = 0 \end{aligned} \quad (7)$$

Thanks to the antisymmetric property of the kernel, the second term in the first integral can be shown to be identical to the first⁵; that is,

$$\int_{-1-a}^{1+a} \Gamma(\sigma) \frac{\partial q_n}{\partial \Gamma}(\delta\Gamma) d\sigma = \int_{-1-a}^{1+a} \delta\Gamma q_n(\sigma) d\sigma \quad (8)$$

The system of equations is quasi-linear and nonhomogeneous. It is solved for a given λ . Then λ is updated using the global identity

obtained by replacing $\delta\Gamma$ with Γ in minimization equation (7), which yields

$$2C_{Di} + C_{Dv1} + 2C_{Dv2} + \lambda C_L = 0 \quad (9)$$

With $\kappa = C_{Ltarget}/C_L$, the new iterate for λ is taken to be

$$\lambda = [2\kappa(C_{Di} + C_{Dv2}) + C_{Dv1}]/C_L \quad (10)$$

It usually requires three or four iterations to obtain the converged solution with the target lift. Note that the inviscid solution is calculated before viscous effects are included.

The inviscid and viscous chord distributions are compared in Fig. 2; both designs have an aspect ratio of $\mathcal{AR} = 10$. The Reynolds number is $Re = 5 \times 10^5$. There is very little difference due to viscous effects: primarily a smaller chord for the winglets. The design incidence is increased to $\alpha = 0.81$ deg and the toe-in angle is not affected. The efficiency factor, however, is significantly decreased when the viscous drag contributions are included. The new value is $e = 1.07$. The circulation and normal wash distributions are shown in Fig. 4. Also shown in Fig. 4 are the elliptic loading distributions. The most significant feature of viscous effects is to bring a positive normal wash on the winglets. This produces a small thrust $C_{Dtw} = -0.000635$ for a friction drag $C_{Dvw} = 0.000953$ on each winglet. The downwash on the main wing is essentially unchanged.

A comparison of the inviscid and viscous designs is also carried out, using the viscous polars of Fig. 5. The results are displayed in Fig. 6. The conclusions are similar to those of the simpler case.

The effect of viscosity is best exemplified by comparing two designs, at high and low Reynolds numbers. The high Reynolds number, $Re = 8 \times 10^6$, has $C_{d0} = 0.00595$, whereas the low Reynolds number, $Re = 50,000$, has $C_{d0} = 0.0119$, a twice larger drag coefficient. The results are presented in Fig. 7. The low-Reynolds-number flow has twice the induced normal wash on the winglets as compared

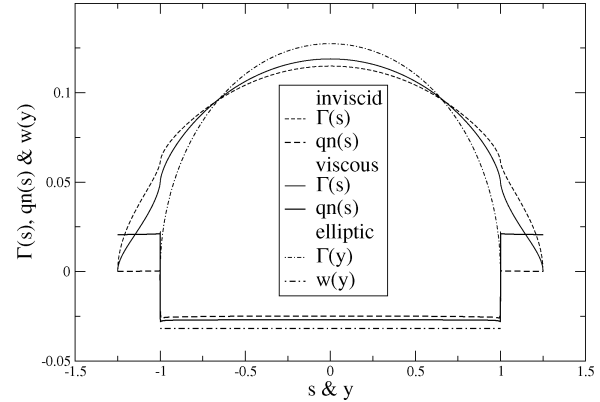


Fig. 4 Distribution of circulation and normal wash using linear lift curve and flat-plate C_d .

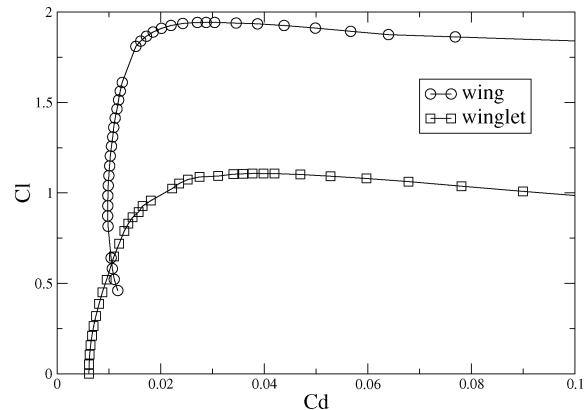


Fig. 5 Viscous polar for wing and winglet, $Re = 5 \times 10^5$ (XFOIL⁷).

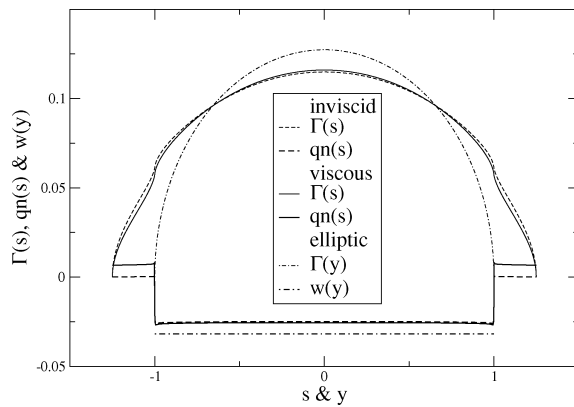


Fig. 6 Distributions of circulation and normal wash using inviscid and viscous polars.

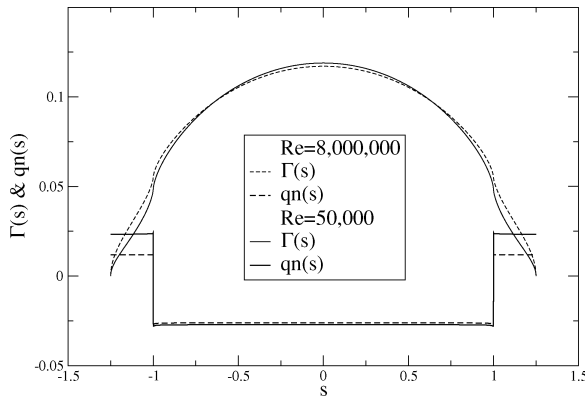


Fig. 7 Effect of Reynolds number on the optimum design.

to the high-Reynolds-number flow. On the main wing, the effect is not significant, as mentioned previously.

Effect of Yaw

It has been shown in Ref. 5, using an inviscid flow model, that the optimum winglets provide weathercock stability when the flow is not aligned with the plane of symmetry of the wing. In the present analysis, as in that of Ref. 5, the vortex sheet is not changed when yaw is added. This is consistent with the small disturbance approximation inherent in the method and is valid only for small yaw angles. The viscous effects result in a decrease of the restoring moment and could possibly destabilize the wing and winglet configuration at large yaw angles. A general statement cannot be made in the viscous case. Hence, a small yaw angle of 1 deg is considered, because the viscous effects have a strong nonlinear behavior with yaw. The results are presented in Fig. 8 for different winglet heights. As can be seen, the restoring moment has almost been reduced by a factor of 2 for the configuration. Again, viscosity primarily affects the winglets in terms of induced drag and yawing moment. It can be concluded, however, that the yaw stiffness, $-\partial N/\partial \text{yaw}$, is positive at zero yaw angle, a necessary requirement for weathercock stability.

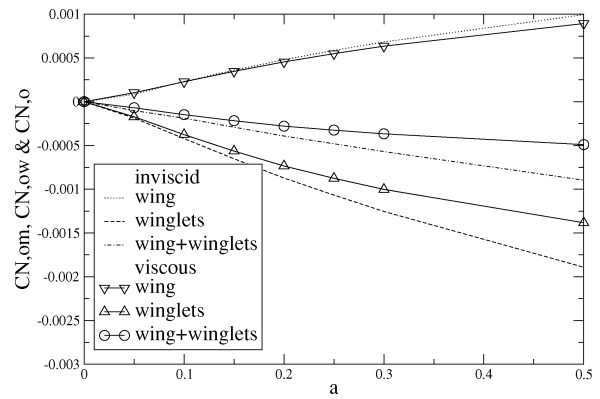


Fig. 8 Effect of winglet height on yawing moment, yaw = 1 deg.

Conclusions

An optimization code, based on the Prandtl lifting line model with inviscid or viscous polars, has been used to find the distribution of circulation and normal induced velocity for a wing/winglet configuration of aspect ratio $AR = 10$ equipped with 25% winglets. It has been found that viscosity has little effect on the optimum geometry; however, it has a significant effect in reducing the efficiency factor. The winglets produce a thrust that counteracts some of the friction drag of the winglets. The upwash on the winglets depends on the partial derivatives $\partial C_d/\partial C_l$ and $\partial^2 C_d/\partial C_l^2$.

The effect of yaw has been investigated and the optimal wing/winglet combinations have been found to have weathercock stability at design conditions, even in the presence of viscous effects.

References

- ¹Prandtl, L., and Betz, A., *Vier Abhandlungen zur Hydro- und Aerodynamik*, Göttingen, Germany, 1927.
- ²Munk, M. M., "The Minimum Induced Drag of Aerofoils," NACA Rept. 121, 1921.
- ³Whitcomb, R. T., "A Design Approach and Selected Wind-Tunnel Results at High Subsonic Speeds for Wing-Tip Mounted Winglets," NASA TN D-8260, July 1976.
- ⁴Ishimitsu, K. K., "Aerodynamic Design and Analysis of Winglets," AIAA Paper 76-940, 1976.
- ⁵Chattot, J. -J., "Analysis and Design of Wings and Wing/Winglet Combinations at Low Speeds," *Computational Fluid Dynamics Journal*, Vol. 13, No. 3, 2004, pp. 597-604.
- ⁶Chattot, J. -J., "Optimization of Wind Turbines Using Helicoidal Vortex Model," *Journal of Solar Energy Engineering*, Vol. 125, No. 4, 2003, pp. 418-424.
- ⁷Drela, M., "XFOIL: An Analysis and Design System for Low Reynolds Number Airfoils," *Low Reynolds Number Aerodynamics*, edited by T. J. Mueller, Lecture Notes in Engineering No. 54, Springer-Verlag, 1989.
- ⁸Chattot, J. -J., "Optimization in Applied Aerodynamics," *Computational Fluid Dynamics Journal*, Vol. 9, No. 3, 2000, pp. 307-311.
- ⁹Kuhlman, J. M., and Liaw, P., "Winglets on Low-Aspect-Ratio Wings," *Journal of Aircraft*, Vol. 25, No. 10, 1988, pp. 932-941.
- ¹⁰Lundry, J. L., and Lissaman, P. B. S., "A Numerical Solution for the Minimum Induced Drag of Nonplanar Wings," *Journal of Aircraft*, Vol. 5, No. 1, 1968, pp. 17-21.

Q3

Q4

Q5

Q6

Queries

- Q1.** Title of paper should be 12 words maximum (hyphenated terms count as two or more words; acronyms not permitted). Please revise.
- Q2.** Unless there's a reason to use a specific type of enclosure, enclosures should go in the order {{{{(...)}}}}. OK as set?
- Q3.** Fig. 8 as meant?
- Q4.** Give publisher.
- Q5.** Give month./If this was subsequently published in an archival source, give full publication information.
- Q6.** Give city of publisher./Give page range or chapter if applicable.